Selective conversion of guaiacol to substituted alkylphenols in supercritical ethanol over MoO₃

Kai Cui [a,b], Le Yang [a,b], Zewei Ma [a,b], Fei Yan [a,b], Kai Wu [a,b], Yushuai Sang [a,b], Hong Chen [c], Yongdan Li [a,b,*]

[a] *State Key Laboratory of Chemical Engineering (Tianjin University), Tianjin Key Laboratory of Applied Catalysis Science and Technology, School of Chemical Engineering, Tianjin University, Tianjin 300072, China*
[b] *Collaborative Innovation Center of Chemical Science and Engineering (Tianjin), Tianjin 300072, China*
[c] *School of Environmental Science and Engineering, Tianjin University, Tianjin 300072, China*

ARTICLE INFO

ABSTRACT

Selective conversion of guaiacol over MoO₃ to produce various alkylphenols, including ethylphenols, isopropylphenols, butylphenols (*tert-*, *sec-*) and *tert*-amylphenol is investigated in ethanol without the addition of gaseous hydrogen. A high conversion of 99% is achieved at 280 °C for 4 h and the total alkylphenols account for up to 94% in the quantified products. Six molecules, *i.e.* 2,5-diethylphenol, 2,6-diisopropylphenol, 2,4-diisopropylphenol, 2,6-ditertbutylphenol, 2,4-ditertbutylphenol and 2,6-ditertbutyl-4-ethylphenol, are the main outcomes. The higher alkylphenols in the aforesaid products are verified to form via a novel reaction step in which hydrogen atom at the α-carbon of the lower alkylphenol is substituted consecutively with methyl or ethyl groups. Further examination reveals that catechol is formed as the intermediate via demethylation of guaiacol and followed by direct conversion to low alkylphenols without the formation of phenol. Post-catalytic analysis indicates that an oxycarbo-hydride phase ($MoO_xC_yH_z$) with Mo^{5+} developed in the supercritical alcohol batch system played the role of active species. Ethanol is found to be the most effective solvent for the conversion. The MoO₃ catalyst undergoes a gradual deactivation resulted from the consumption of Mo^{5+} and carbon deposition but can be regenerated with a simple calcination.

© 2017 Elsevier B.V. All rights reserved.

1. Introduction

Lignin is considered as the major aromatic source of the bio-based economy [1]. However, due to the high oxygen content and instability of the primary products, the effective utilization of lignin is still a challenge [2]. Recently, lignin was converted into value-added small-molecular chemicals in the presence of common alcohols with combining the depolymerisation and upgrading reactions in a single step [3–12]. For example, catalytic disassembly of lignin into monomeric cyclohexyl derivatives was reported by Barta et al. with a Cu-based mixed metal oxide catalyst in supercritical methanol without addition of H₂ [3]. Ma et al. [4] achieved the complete ethanolysis of Kraft lignin in supercritical ethanol over an α-MoC$_{1-x}$/AC catalyst, giving a remarkably high yield of aliphatic

and aromatic chemicals without char and tar formation. Huang et al. [6] afterwards utilized a CuMgAlO$_x$ catalyst in the valorization of soda lignin in supercritical ethanol to produce aromatic small molecules. More recently, Narani et al. [9] presented a method of catalytic hydrotreatment of Kraft lignin to a number of alkylphenolics with high selectivity using supported NiW and NiMo catalysts in supercritical methanol. However, the reaction pathways of the lignin upgrading processes are still unclear. Especially, the origin of stable higher alkylphenol products, such as isopropylphenols [6] and butylated hydroxytoluene (BHT) [7,9], becomes a curious question. Catalytic conversion of lignin-derived model compounds in alcohols and the exploration of the reaction mechanisms may give the solution.

Guaiacol, containing simultaneously hydroxyl and methoxyl groups, has been often chosen as a lignin model compound because the guaiacyl unit is a primary structure in lignin [13]. Early works indicated that traditional NiMoS₂, CoMoS₂ catalysts [14–16] and supported metal catalysts, including noble metals such as Ru, Rh, Pd, Pt [17–20], as well as base metals such as Ni, Co, Fe and their alloys [21–24], are active for the hydrodeoxygenation (HDO) of

guaiacol in aqueous phase or in nonpolar solvents (*n*-decane or *n*-hexadecane). However, these catalysts require high H_2 pressure and temperature. Otherwise, they often experience rapid deactivation and easy ring saturation. A stable catalyst selectively cleaving the C—O bond of guaiacol under mild conditions is still called for.

To avoid the use of external hydrogen, several new processes were proposed. The hydrolysis of guaiacol has been investigated in a water system with HCl or water-tolerant Lewis acids, *e.g.* In(OTf)$_3$, Sc(OTf)$_3$, Yb(OTf)$_3$, In(Cl)$_3$, as catalysts in 225–280 °C without H_2 pressure [25,26]. Catechol was obtained mainly from a charged intermediate formed via the protonation effect of water and acid, nevertheless, no deoxygenated products were observed. Alternatively, alcohols were also applied as a hydrogen-donor solvent in the conversion of guaiacol [27,28]. As a representative, combined selectivity of up to 85% for phenol and ethylphenols with a guaiacol conversion of 87% was achieved at 340 °C over an α-MoC$_{1-x}$/AC catalyst. The reaction takes place via demethylation followed by deoxygenation and transalkylation [28]. In comparison, catalytic HDO of guaiacol in alcohol media is more favorable than hydrolysis in water due to the selective and effective oxygen-removal.

On the other hand, transition metal phosphides, nitrides, carbides and oxides, featuring high selectivity to aromatics and outstanding poison resistance, have been intensively explored in lignin derivatives upgrading [29–37]. Among them, MoO$_3$ is regarded as a promising catalyst due to its good specific rates for HDO reaction [29,33,36,37]. Recently, Prasomsri et al. [33] demonstrated that MoO$_3$ effectively catalysed the HDO of various biomass-derived oxygenates, *i.e.* aliphatic and cyclic ketones, furanics, and phenolic feeds, to unsaturated hydrocarbons under a low H_2 pressure. In their following work, MoO$_3$ was used to selectively cleave the C—O bond of guaiacol in the vapour-phase at 350 °C under 0.1 MPa pressure ($P_{Reactant+H2}$). Aromatic hydrocarbons and phenol were produced with yields of 44.6% and 29.3%, respectively [36]. Shetty et al. [37] reported the preferential stabilization effect of the support, *i.e.* SiO$_2$, γ-Al$_2$O$_3$, TiO$_2$, ZrO$_2$ and CeO$_2$, on the Mo oxidation states in the deoxygenation of *m*-cresol under similar reaction condition. These important contributions indicate the possibility for MoO$_3$ to perform excellent HDO activity in moderate conditions.

Herein, the supercritical ethanol solvent and MoO$_3$ catalyst are combined in the guaiacol transform process. A number of higher alkylphenols, six molecules as the main products, are formed with high conversion and selectivity at a relatively low temperature, 280 °C, under N_2 atmosphere. The reaction pathway of guaiacol to higher alkylphenols in supercritical ethanol via selective deoxygenation and consecutive substitutions is proposed. An oxycarbohydride phase with pentavalent molybdenum is further found responsible for the reaction activity, and it is synthesized with the assistance of active hydrogen species (not H_2) from supercritical alcohol. Based on it, the reason for different deoxygenation activities in alcohols is revealed.

2. Experimental

2.1. Materials

The analytical reagent grade chemicals and solvents including molybdenum (VI) trioxide, guaiacol, ethanol, methanol, isopropanol, *n*-hexane, hexahydrotoluene, catechol, resorcinol, anisole, phenol and *o*-cresol were purchased from Tianjin Guangfu Technology Development Co., Ltd. Molybdenum (IV) dioxide (99% metal basis) and 2-isopropylphenol (98%) were obtained from Alfa Aesar. Adamas Reagent Co., Ltd. provided 4-ethylphenol (99%+). These materials were directly used as received.

2.2. Activity measurements

In a typical experiment, guaiacol (2.0 g), ethanol (100 ml) and MoO$_3$ (0.5 g) were added into a Parr 4566 reactor (300 ml). The reactor was purged with N_2 and heated to the reaction temperature (220–300 °C) with stirring at 600 rpm. After reaction, the reactor was rapidly cooled to room temperature. The liquid products and the catalyst were recovered and separated. All the liquid products were analysed and quantified using the internal standard method with a gas chromatograph equipped with a flame ionization detector (GC-FID, Agilent Technologies, model 6890) and a HP-5 MS capillary column (Agilent, 30 m × 0.25 mm × 0.25 μm). For the liquid products obtained in ethanol and isopropanol, *o*-cresol was chosen as an internal standard. For the liquid products in methanol, *n*-hexane and hexahydrotoluene, anisole was used as the internal standard. The relative correction factors were obtained using the formulae taking account the effective carbon number and the molecular weight. The GC parameters used for the analysis were: injector temperature 280 °C; detector temperature 300 °C; split ratio 50:1. The oven temperature program was set from an initial temperature of 45 °C to a final temperature of 250 °C at 10 °C/min, and then held at the final temperature for 2 min. The products were identified using a mass selective detector (MSD, Agilent Technologies, model 5973) with the aid of the National Institute of Standards and Technology (NIST) library. Molecules with higher molecular weight in liquid products were analysed by full-scan electrospray ionisation mass spectrometry (*m/z* range from 250 to 850) on an Agilent 6310 Ion Trap. Besides, the gaseous products were analysed using a GC equipped with two packed columns. H_2, N_2, CO, CO_2 and CH_4 of the gases were separated by a TDX-01 packed column (2m) and analysed with a thermal conductivity detector (TCD). Other products of the gases were verified using a Porapak Q colum (3 m) connected to a FID. Because the quantified liquid products each consume one mol of guaiacol, the conversion (C (%)), the product specific selectivity (S (%)) and the mass balance (M (%)) were calculated according to Eqs. (1)–(3).
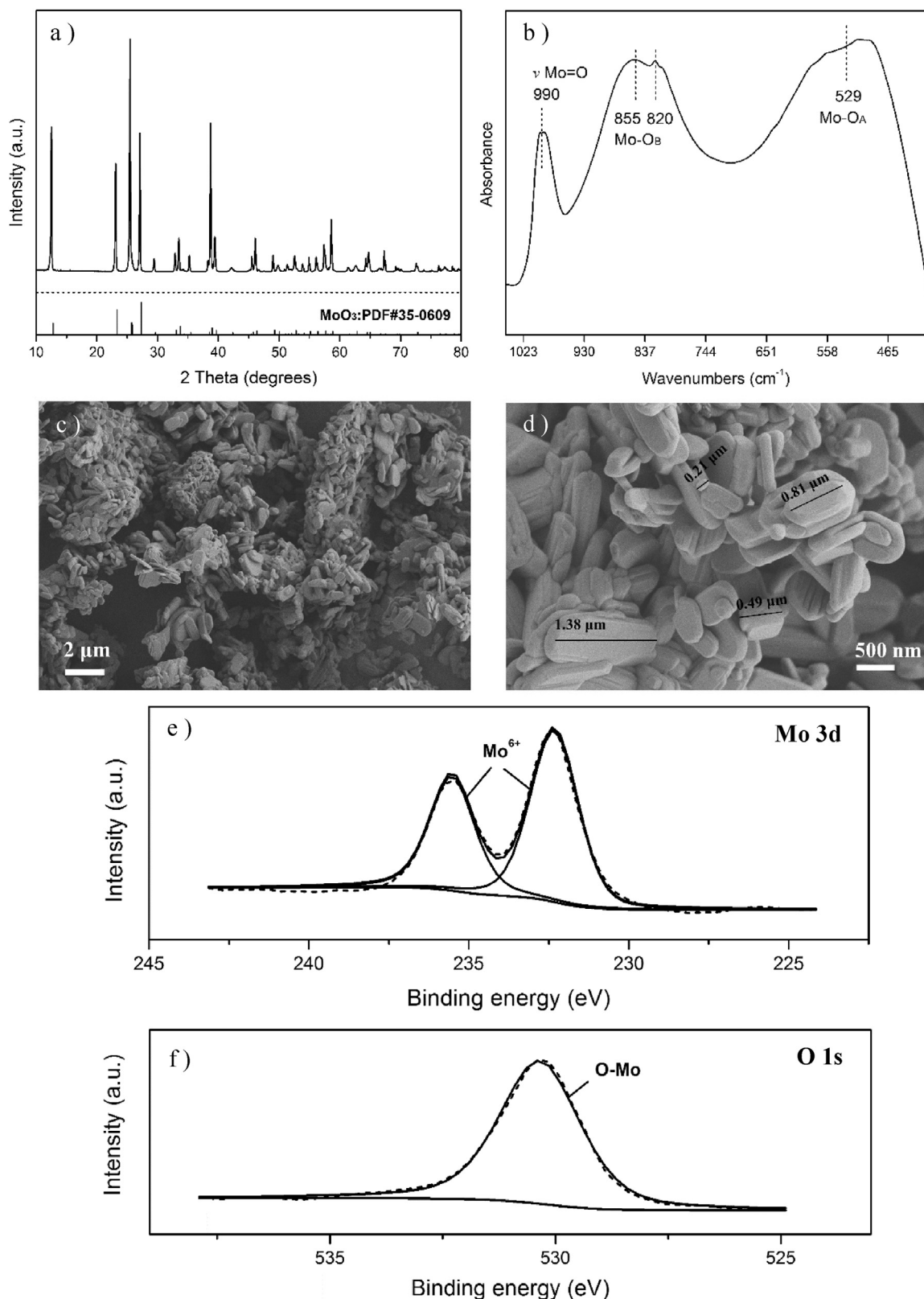
$$C\,(\%) = \frac{n(Guaiacol)_{initial} - n(Guaiacol)_{residual}}{n(Guaiacol)_{initial}} \times 100\% \quad (1)$$

$$S\,(\%) = \frac{n\,(Product)}{n(Guaiacol)_{consumed}} \times 100\% \quad (2)$$

$$M\,(\%) = \sum S_{i_{quantified products}} \quad (3)$$

2.3. Characterization

The structure of the catalyst samples was identified with an X-ray diffraction (XRD) technique (Bruker AXS, D8-S4), operated at 40 kV and 40 mA, using a Cu-Kα monochromatized radiation source. Scans were done between 2θ of 10° and 80° at a rate of 3.5° min^{-1}. N_2 physisorption isotherms were recorded with a Quantachrome Autosorb-1. Prior to measurement, the samples were degassed under vacuum at 250 °C for 6 h. The specific surface area of the catalyst was measured using the BET method at relative pressures (P/P$_0$) ranging from 0.05 to 0.30. The total pore volume was derived from the adsorption amount at a relative pressure of 0.99. Fourier transform Infrared (FT-IR) spectra were collected at room temperature on a Nexus spectrometer (Thermo Nicolet Co.) with a resolution of 4 cm^{-1} for 32 scans in the region 4000–400 cm^{-1} and the pellets were prepared by mixing 10 mg of sample in 150 mg KBr. Raman spectra were obtained with a Renishaw inVia reflex spectrometer. Approximately, 50 mg of sample was analysed under a 532 nm He-Ne laser excitation source. The X-ray photoelectron spectroscopy (XPS) was performed with a PHI-1600 ESCA system spectrometer using Mg Kα as the X-ray source

Fig. 1. a) XRD pattern, b) FT-IR spectrum, c) d) SEM micrographs, e) f) XPS spectra of the fresh MoO_3 catalyst.

(1253.6 eV) under a residual pressure of 5×10^{-6} Pa, with the binding energy calibrated using C1s at 284.6 eV as the standard. The scanning electron microscope (SEM) micrographs were taken with a Zeiss SUPRA 55 SAPPHIRE microscope with acceleration voltage of 2 kV. The atomic mapping measurements were performed on Oxford X-max EDS attachments with an acceleration voltage of 15 kV. High-resolution transmission electron microscopy (TEM) was carried out on a JEOL-JEM-2100F electron microscope operating at 200 kV. Before observation, the sample was ultrasonically
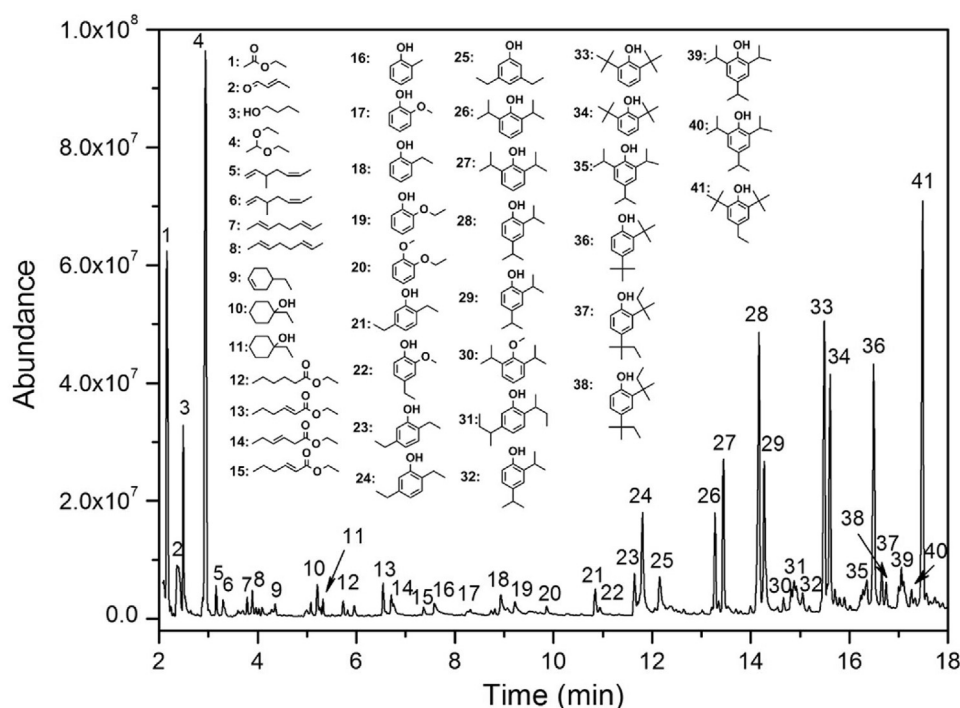
Fig. 2. The TIC of the liquid product of guaiacol conversion at 280 °C for 4 h in ethanol.

suspended for 30 min and then deposited onto a copper grid coated with a carbon film.

3. Results and discussion

3.1. Catalyst before reaction

The XRD pattern in Fig. 1a depicts that the structure of the unused MoO_3 is consistent with the orthorhombic molybdenum trioxide (PDF#35-0609). Three types of connections between Mo and O atoms are detected, as shown in Fig. 1b, with the FT-IR [38]. The broad and complex band centred at about 529 cm^{-1} is due to the stretching vibration of the O_A atoms each linked to three Mo atoms. The absorption patterns with two maxima at 855 cm^{-1} and 820 cm^{-1} come from the vibration of the O_B atoms in Mo-O-Mo entities. A band at 990 cm^{-1} is clearly observed and is attributed to the vibration of the terminal oxygen in Mo=O. The SEM micrographs reveal that the MoO_3 particles aggregate to bulk and have a platelike morphology with sizes in the range of 0.2–1.4 μm (Fig. 1c and d). The surface area and average pore volume of the fresh catalyst were measured as 3.27 m^2 g^{-1} and 2.79 × 10^{-3} cm^3 g^{-1}, respectively. Similarly, Matsuda et al. reported that bulk MoO_3 has a low surface area of 5 m^2 g^{-1} [39]. Fig. 1e presents the surface XPS spectrum of Mo species, showing only the existence of Mo^{6+} with two well-resolved peaks at binding energies (BEs) of 233.2 and 236.3 eV assigned to the Mo 3d$_{5/2}$ and 3d$_{3/2}$ spin-orbit components. The only O 1s peak located at 530.4 eV is perfectly symmetrical and attributed to oxygen bonded to metal (Fig. 1f).

3.2. Product analysis

A clear liquid was obtained after reaction under N_2 atmosphere at 280 °C for 4 h. Table S1 gives the distribution of gas products, showing a certain amount of H_2, CO, CH_4, C_2H_4, C_2H_6 and a small amount of CO_2, C_3H_6, C_3H_8, $C_4H_{10}O$ (diethyl ether) were formed in the process. The total-ion chromatogram (TIC) derived from the gas chromatograph-mass spectrometer (GC–MS) for the liq-

uid products is presented in Fig. 2. Forty-one molecules (P1-41) were identified after the reaction. P1-15, including esters, alcohols and olefins, were verified to be formed from ethanol by heating ethanol and MoO_3 under the same conditions. Except the internal standard of o-cresol (P16) and the reactant of guaiacol (P17), the other 24 aromatic molecules (P18-41) were only measured in the product with addition of guaiacol. The results of the factorial reactions, focusing on the 24 products from guaiacol, are listed in Table 1 and the pressures recorded are given in Table S2. Alkylphenols such as ethylphenols (EPs), isopropylphenols (IPPs), tert- or sec- butylphenols (BPs) and tert-amylphenol (TAP), formed via deoxygenation and consecutive alkylation, were obtained as the dominating products with a high combined selectivity. Meanwhile, a small amount of o-ethoxy phenol (OEP) via transetherification [27], p-ethyl guaiacol (PEG) and alkylation & dehydroxylation products (ADPs) were also observed. No completely deoxygenated products or ring hydrogenation products were detected. Full-scan electrospray ionisation mass spectrometry (ESI–MS) analysis verified the existence of trace amount of molecules with higher (exceed 250 g/mol) molecular weight (Fig. 3). These results are distinctly different from those reported in early works, where completely deoxygenated and ring-saturated products were obtained over $CoMoS_2$, Rh, Co etc. catalysts [14,17,23]. Besides, only EPs were detected over the α-MoC_{1-x}/AC catalyst in supercritical ethanol [28]. Here, MoO_3 shows a remarkable selectivity to partial deoxygenation and higher alkylphenol production.

3.3. Effect of reaction conditions

The reaction temperature and time were examined in the ranges of 220–300 °C and 1–5 h (Table 1, Entry 1–11), respectively, in ethanol. At 220 °C (Table 1, Entry 1), the reaction almost did not happen. A low conversion of 8% was observed when the temperature was increased to 240 °C (Table 1, Entry 2), but more than half of the products were not deoxygenated. Until 260 °C (Table 1, Entry 3), the deoxygenated alkylphenols became the main products and the ethanol solvent has been in the supercritical state (Table S1).

Table 1
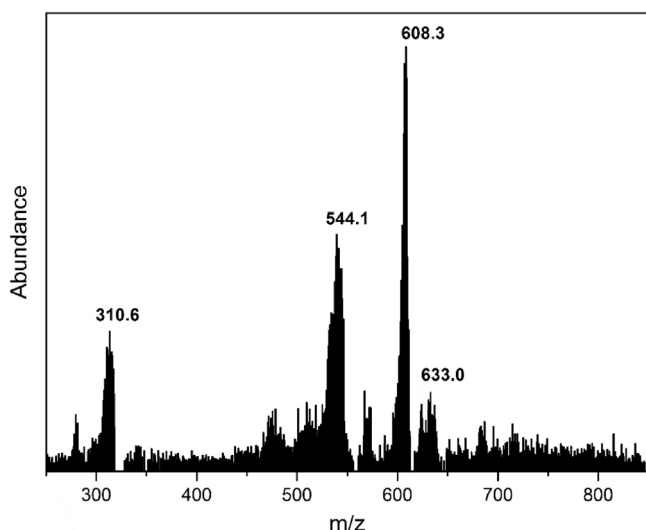Catalytic results of guaiacol conversion in ethanol under different conditions [a].

Entry	T/°C	t/h	M[c]/%	C[d]/%	S[e]/%						
					EPs	IPPs	BPs	TAP	OEP	PEG	ADPs
1	220	4	–	–	–	–	–	–	–	–	–
2	240	4	94	8	3	15	21	–	17	20	18
3	260	4	90	70	20	28	28	1	8	2	3
4	270	4	89	93	19	30	32	1	4	1	2
5	280	4	92	99	19	30	35	2	3	1	2
6	290	4	91	99+	17	32	37	2	1	–	2
7	300	4	90	99+	16	29	38	1	2	1	3
8	280	1	88	65	23	24	26	–	10	2	3
9	280	2	86	80	19	24	28	1	8	2	4
10	280	3	91	94	18	29	33	1	5	2	3
11	280	5	86	99	19	28	30	2	3	1	3
12[f]	280	4	90	99	21	29	34	1	2	1	2
13[g]	280	4	89	78	55	25	4	–	–	–	5
14[h]	280	4	92	40	–	5	87	–	–	–	–
15[i]	280	4	93	2	45	–	–	–	–	–	48
16[j]	280	4	94	5	–	–	–	–	59	35	–
17[k]	280	4	86	78	30	22	13	–	16	5	–
18[l]	280	4	92	40	28	23	13	–	20	8	–
19[m]	280	4	90	34	32	21	11	–	20	6	–
20[n]	280	4	92	99	12	28	45	3	2	–	2

[a] Reaction conditions: guaiacol (2.0 g), catalyst (0.5 g), solvent (100 ml), initial 0 MPa N_2 pressure, and the yields were calculated by moles. [b] A. & D.: alkylation and dehydroxylation. [c] M: mass balance. [d] C: conversion. [e] S: selectivity (EPs: ethylphenols, IPPs: isopropylphenols, BPs: *tert-* or *sec-* butylphenols, TAP: *tert-*amylphenol, OEP: *o*-ethoxy phenol, PEG: *p*-ethyl guaiacol, ADPs: alkylation and dehydroxylation products). [f] Reaction conducted in 1 MPa H_2. [g], [i] Reactant used was 4-ethylphenol. In these cases, product EPs does not include 4-ethylphenol. [i] No catalyst applied. [h] 2-isopropylphenol was used as the reactant. In this case, product IPPs does not include 2-isopropylphenol. [j], [n] Catalysts used in Entry 16 and 20 were MoO_2 and regenerated MoO_3 by calcination, respectively. [k], [l], [m] First reuse, second reuse and third reuse without treatment.

Table 2
Product distribution of guaiacol in different solvents[a].

Entry	M[b]/%	C[c]/%	S[d]/%							
			P	MPs	EPs	IPPs	tert-BPs	MTPs	AGs	ADPs
21[e]	61	94	–	29	–	4	20	–	6	2
22[f]	95	94	–	–	–	59	2	1	5	28
23[g]	96	2	30	7	2	–	–	20	15	22
24[h]	95	4	8	3	2	–	–	26	42	14
25[i]	65	92	–	31	–	4	21	–	6	3
26[j]	96	91	–	–	–	59	3	1	3	30

D[k][e]
D[i]

D[f]
D[j]

D[g]

D[h]

[a] Reaction conditions: see Entry 5 in Table 1. [b] M: mass balance. [c] C: conversion. [d] S: selectivity of each product (P: phenol, MPs: methylphenols, MTPs: methoxyl transetherification products, AGs: alkyl guaiacols). [e], [f], [g], [h] solvents used were methanol, isopropanol, *n*-hexane, hexahydrotoluene, respectively. [i], [j] methanol and isopropanol were used as solvents with the addition of 1 MPa hydrogen. [k] D: detail product composition.

Fig. 3. ESI–MS analysis of the liquid products at 280 °C for 4 h in ethanol (*m/z* range from 250 to 850).

As the temperature increased sequentially (Table 1, Entry 4–7), the guaiacol could almost be converted completely with a conversion of 99% at 280 °C. For the reaction time (Table 1, Entry 5, 8–11), the conversion of 99% was obtained until it increased to 4 h. In addition, the increase in the reaction temperature (260–300 °C, Table 1, Entry 3–7) and time (1–5 h, Table 1, Entry 5, 8–11) resulted in a certain improvement for the selectivities of IPPs, *tert*- and *sec*- BPs and TAP, and a lower selectivity towards EPs, indicating that EPs may be intermediate products to the higher alkylphenols. However, the change in selectivity was moderate. At 280 °C and with 4 h, the total selectivity of 86% towards the alkylphenols with a conversion of 99% was accepted (Table 1, Entry 5). For the quantified products, the alkylphenols account for about 94%, and six molecules assigning to the ten intense peaks in the TIC (Fig. 2, peak 23, 24, 26, 27, 28, 29, 33, 34, 36, 41), *i.e.* 2,5-diethylphenol, 2,6-diisopropylphenol, 2,4-diisopropylphenol, 2,6-ditertbutylphenol, 2,4-ditertbutylphenol and 2,6-ditertbutyl-4-ethylphenol, were the main products. The total solvent consumption in converting 2.0 g of guaiacol is about 11% of added ethanol in the reaction.
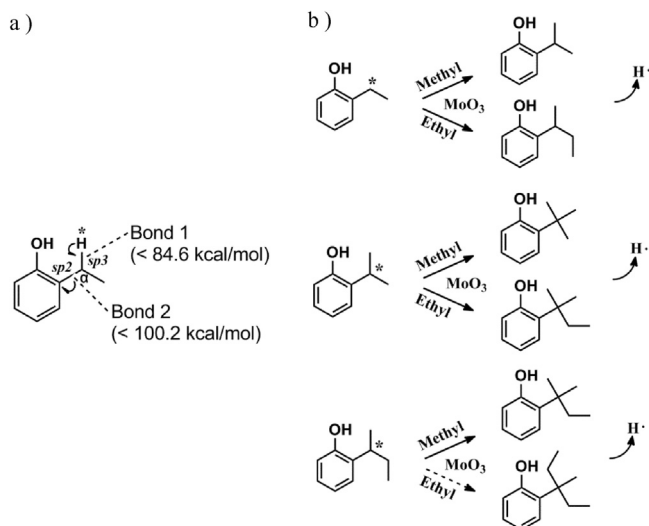
The conversion of guaiacol was also tested using various solvents (Table 2). There were no EPs, *sec*-BPs or TAP found in methanol and isopropanol, though they facilitated high conversion of guaiacol, both 94% (Table 2, Entry 21–22). Instead, methylphenols (MPs) and *tert*-BPs were formed mostly in methanol, and IPPs were produced as the main alkylphenols in isopropanol. The diversity of alkylphenol products in ethanol should be due to its unique reactivity, *i.e.* the capacity to create methyl and ethyl groups simultaneously in the reaction medium. The ability has been stated in the work of Chen et al. [40]. Notably, when guaiacol was reacted in methanol at 280 °C for 4 h in the presence of the catalyst, a faint yellow floccule was formed. Quantitative analysis based on GC showed that the mass balance of products was only 61% (Table 2, Entry 21). The same phenomenon was reported by Huang et al. over a CuMgAlOₓ catalyst [41]. They proved that significant oligomerization takes place in methanol because methanol can be readily converted to formaldehyde with metal catalysts, which accelerates the polymerization of phenols to phenolic resin. Hence, the main conversion of guaiacol in methanol in this work is involved not only with selective deoxygenation reaction but also with polymerization reaction. For isopropanol, the deoxygenation degree (proportion of alkylphenols in quantified products) was not as good as in ethanol (94%) and methanol (87%). More than 30% products were not deoxygenated (Table 2, Entry 22). The conversion

of guaiacol in isopropanol therefore gives the products of selective deoxygenation and side-reactions without deoxygenation. In *n*-hexane and methylcyclohexane, undesired products, such as *o*-ethoxy phenol, 3-methyl guaiacol and *o*-dimethoxy benzene, were obtained as the major products at low conversions of 2% and 4% (Table 2, Entry 23–24). Phenol (P), MPs and EPs also appeared without upgrading to higher alkylphenols. Obviously, these are not good solvents for guaiacol conversion. In summary, we conclude that MoO₃ performs a good activity for guaiacol conversion in alcohol solvents, especially in ethanol.
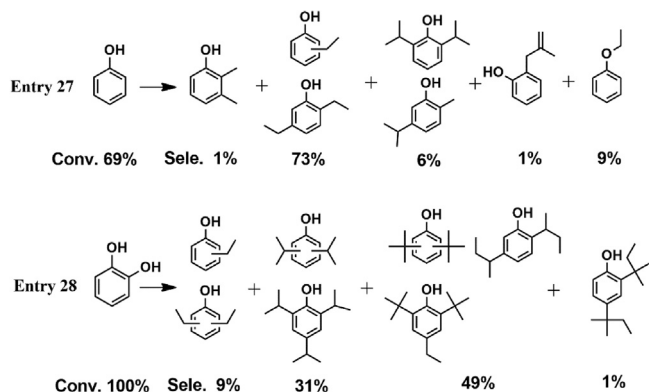
Further, 1 MPa hydrogen was applied to the reactions in alcohol solvents (ethanol, methanol and isopropanol, Table 1, Entry 12, Table 2, Entry 25–26). Under the conditions, all solvents are in supercritical states, which insures the good dissolution of hydrogen molecule. Nevertheless, the reactions gave similar conversions and product selectivities to the reactions under N₂ (Table 1, Entry 5, Table 2, Entry 21–22). Even the final gas pressure after the reactions is about 1 MPa more than that without the addition of hydrogen (Table S1). It is consistent with the results of lignin valorization by Song et al.[42], in which the similar performances were observed in methanol with H₂ and Ar, respectively. This suggests that the dominating active hydrogen species during the reaction may not be the gaseous hydrogen. That is, the active hydrogen species comes from the supercritical alcohols. From the thermodynamics point of view, the transformation of alcohol to active hydrogen species is easier than gaseous hydrogen due to the high bond dissociation energy (DE) of the H—H bond (104.2 kcal mol⁻¹) in H₂ [43]. The study of Wang et al. for upgrade of phenolic and aromatic biorefinery feeds with RANEY Ni also showed the same evidence [44].

3.4. Pathways of lower alkylphenols to higher ones

The above-reported results imply EPs are likely to be the precursors of higher alkylphenols in the ethanol system. Considering no isopropyl, butyl (*tert*-, *sec*-) and tertpentyl derived aliphatic compounds and *n*-propyl, butyl (*n*-, *iso*-), pentyl (except tert-pentyl) substituted phenols were detected in the liquid product (Fig. 2), and only rather small amount of propane and propylene (0.3%) possibly derived from isopropyl was observed in the gaseous product (Table S1), we postulate that the higher alkylphenols were more likely to form via consecutive substitution of lower alkylphenols with methyl or ethyl groups supplied by ethanol medium, instead of via direct substitution with corresponding substituent groups or isomerization with interrelated alkylphenols. Reactions with 4-ethylphenol and 2-isopropylphenol as reactants were tested under the same conditions. The elevated products, IPPs and *tert*-BPs (Table 1, Entry 13, 14), revealed that the higher alkylphenols are formed from lower alkylphenols. Taking the formation of IPPs as an example, isomerization is not feasible due to the absence of *n*-propylphenols in the product, so they should be from the direct conversion of EPs. EP contains two types of relevant bonds with different DEs, Bond 1 (DE < 84.6 kcal/mol) and Bond 2 (DE < 100.2 kcal/mol), as shown in Scheme 1a [45,46]. The ethyl can be converted to isopropyl via either (I) breakage of Bond 1 accompanied by methyl attachment or (II) cleavage of Bond 2 accompanied by isopropyl addition. The former path happens easier due to the lower DE of Bond 1. The available methyl and ethyl in supercritical ethanol also effectively facilitate the approach (I). Based on it, Scheme 1b represents the preliminary reaction pathways of lower alkylphenols to higher alkylphenols. The carbon atom located at benzene ring of EP, with electrons in sp² hybridized orbits, has a furious inducement effect to electrons in sp³ hybridized orbits of α-carbon, which attracts the adjacent hydrogen electron and leads the H atom to be activated (Scheme 1a). Thus, EP can transform to IPP or *sec*-BP preferentially via losing the activated hydrogen on α-carbon under the contact of methyl or ethyl. In the same way, IPP is

Scheme 1. a) Relevant bond analysis of EP. b) Reaction pathways of lower alkylphenols to higher alkylphenols. *: Activated atom.
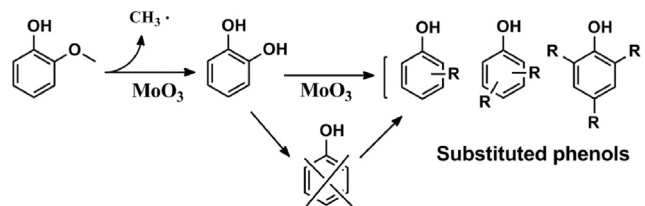

Scheme 2. Conversion of guaiacol potential reaction intermediates over MoO$_3$ in supercritical ethanol. Reaction conditions: reactant (2.0 g), catalyst (0.5 g), time (4 h), temperature (280 °C), ethanol (100 ml), initial 0 MPa N$_2$ pressure, and the yields were calculated by moles.

converted to *tert*-BP and TAP, and *sec*-BP is turned to TAP and *tert*-hexylphenol. Of course, substitution reactions on benzene rings also happen concurrently. GC analysis further confirms the existence of the above products in the system except *tert*-hexylphenol due to its trace amount and high molecular weight. Entry 15 forms small amounts of EPs and no higher alkylphenols were observed in the absence of a catalyst, suggesting MoO$_3$ is essential to the consecutive substitutions.

3.5. Pathways of guaiacol to lower alkylphenols

Several possible reaction intermediates, phenol, catechol and anisole, were tested as reactants to further understand the reaction pathways (Scheme 2). Anisole didn't show activity at 280 °C for 4 h. Phenol was converted to mainly EPs with a selectivity of 73% at a conversion of 69%. Minor products of MPs, IPPs, isobutylenephenols and phenetole were also detected, accounting for 1%, 6%, 1% and 9%, respectively (Scheme 2, Entry 27). For catechol, complete conversion was achieved to produce EPs, IPPs, BPs (*tert*-, *sec*-) and TAP with selectivities of 9%, 31%, 49% and 1%, respectively (Scheme 2, Entry 28), which was in accordance with that obtained with guaiacol as the starting material. These results imply that catechol, via demethylation of guaiacol, should be generated primarily as an intermediate. In contrast, Jongerius et al. [47] reported guaiacol
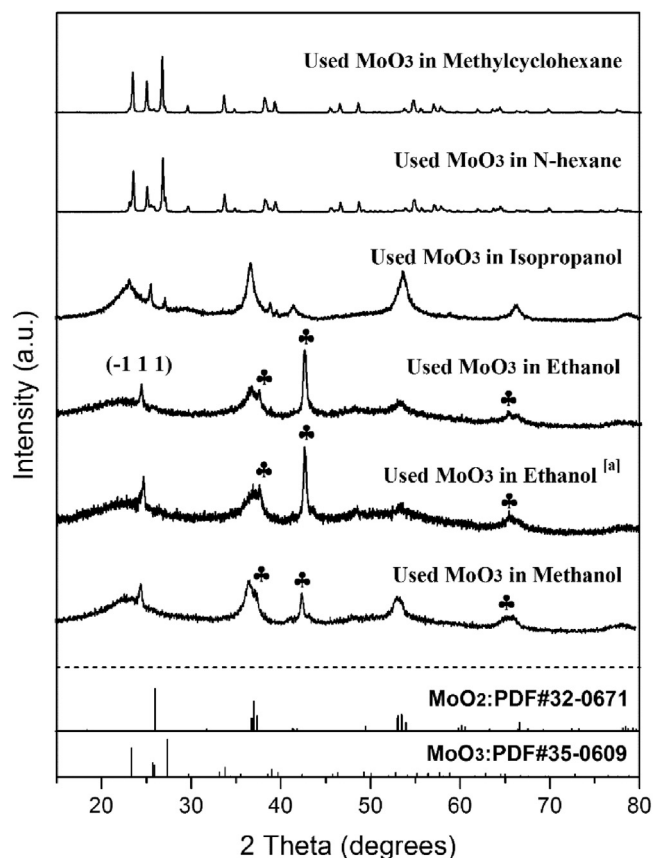

Scheme 3. Transformation pathways of guaiacol in ethanol (R: ethyl, isopropyl, tertbutyl, secbutyl and tertpentyl). Reaction conditions: see Scheme 2.

was directly demethoxygenated to phenol on Mo$_2$C/CNF. Puente et al. [48] observed both phenol and catechol formation, and proposed that phenol was then transformed to other products over CoMoS$_2$/AC. We recently proved catechol was an initial product followed by the hydroxyl group removal to form phenol over α-MoC$_{1-x}$/AC [28]. In this work, phenol was never found in products and this cannot be explained by complete conversion (Scheme 2, Entry 27). Therefore, the reaction pathways are proposed that catechol is formed as the intermediate via demethylation of guaiacol and followed by consecutive substitutions to alkylphenols without the formation of phenol (Scheme 3). The conversion of resorcinol over MoO$_3$ and another conversion of catechol without catalyst were also tested. Neither of them achieved effective deoxygenation to alkylphenols (Scheme S1, Entry 29–30), indicating the process of converting catechol to alkylphenols is based on the interaction between two adjacent hydroxyl groups and the catalyst surface.
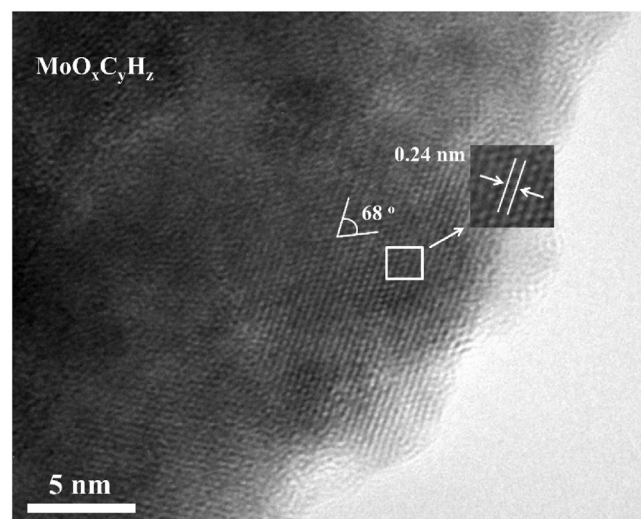
3.6. The active species

The excellent activity of MoO$_3$ drove us to explore the active species in the system. In *n*-hexane and methylcyclohexane, the activities of the catalyst were very low (Table 2, Entry 23–24), and the recovered catalysts showed MoO$_3$ XRD pattern (Fig. 4), suggesting that MoO$_3$ is unlikely the active species. However, in ethanol and methanol (Table 1, Entry 5 and Table 2, Entry 21), the catalyst showed a high activity and did not show a MoO$_3$ XRD pattern after reaction (Fig. 4). Instead, only MoO$_2$ and a special phase were identified for the recovered catalysts, suggesting that either MoO$_2$ or the other phase is the active species. The XRD pattern of the special phase is in accordance with the molybdenum oxyhydride phase (MoO$_x$H$_y$) synthesised via isothermal activation of MoO$_3$ with pure hydrogen at 350 °C by Bouchy et al. [49], however with a small misregistration to the left. Bouchy et al. proved that the MoO$_x$H$_y$ can rapidly pick up carbon to form isostructural oxycarbohydride (MoO$_x$C$_y$H$_z$) in the presence of a carbon source and the cell parameter increases with the extension of the carburation degree [49,50]. Therefore, in the carbonaceous ethanol system, the phase we found should be MoO$_x$C$_y$H$_z$. The misregistration to the left of XRD pattern, indicating the cell parameter increases, confirms the penetration of carbon. Similarly, the (-111) diffraction of MoO$_2$ also shift to the left slightly. For MoO$_x$C$_y$H$_z$, it is possible to measure an interplanar distance of 0.23 ± 0.01 nm for two families of planes making an angle of nearly 70° from the pseudohexagonal symmetry part [50]. The TEM of used catalyst further shows the existence of MoO$_x$C$_y$H$_z$ with the interplanar distance of 0.24 nm and angle of 68° (Fig. 5). A control experiment was made with MoO$_2$ and only 5% conversion was achieved (Table 1, Entry 16), implying that the MoO$_x$C$_y$H$_z$ phase played the role of active component. This is different from previous results, that a dissociative molybdenum ethoxide (Mo(OEt)$_5$) or a molybdenum suboxide (Mo$_4$O$_{11}$) undertook the duty of HDO [29,51]. Overall, the active species of Mo are within the scope of Mo^{6+}, Mo^{5+} and Mo^{4+}. In this work, MoO$_2$ has been proved to be inactive, and MoO$_3$ was not detected after reaction. Therefore, we postulate that Mo^{5+} is responsible for the excellent performance of guaiacol conversion. XPS of a used MoO$_3$ sample after 1 circle in

Fig. 5. TEM image of the $MoO_xC_yH_z$ phase. The inset is the amplification of the framed area.

Fig. 4. XRD patterns of the used catalyst samples. ♣: $MoO_xC_yH_z$ phase. [a]: a blank test without guaiacol in the feed. All the used catalysts were obtained from reactions at 280 °C for 4 h.

ethanol shows the Mo (3d) energy region indeed contains a large amount of Mo^{5+} (56%) with the $3d_{5/2}$ and $3d_{3/2}$ bands locating at 230.9 eV and 234.1 eV, respectively (Fig. 6a). The O 1s XPS spectrum (Fig. 6b) also shows the presence of more than one peak. Except the oxygen bonded to metal at 530.4 eV, the second O 1s peak at 532.5 is attributed to O atoms bonded to carbon [52]. Integration with the results of XRD and XPS, it is likely that the oxycarbohydride phase with Mo^{5+} facilitates the conversion of guaiacol efficiently in supercritical ethanol over MoO_3. A blank test without guaiacol in the feed was carried out. The spent catalyst shows the consistent XRD patterns with those obtained in normal tests (Fig. 4). Similarly, the Mo^{5+} species of close to 50% is observed in catalyst surface (Fig. S1). These results indicate that the alcohol solvent makes a major contribution to the formation of active species.

Prasomsri et al. [36] also reported that the stability and HDO selectivity were improved when a $MoO_xC_yH_z$ phase was present in MoO_3. In their work, guaiacol was converted to phenol and benzene with a conversion of 74.2% at 320 °C in a vapour-phase packed-bed flow reactor under gaseous hydrogen. Here, guaiacol was converted to alkylphenols with a conversion of 99% at a lower temperature of 280 °C in a batch reactor under supercritical ethanol without gaseous hydrogen, which is more suitable for future lignin conversion [4,12,51] due to the solvent alcoholysis for lignin and the mass transfer limitation of lignin in packed-bed flow reactor. Prasomsri et al. proposed that the H_2 pre-reduction is essential to activate the MoO_3 surface. However, our results exhibit molecular H_2 is not indispensable for the conversion and the active hydrogen species from alcohols seems to be the real hydrogen source. Early work on temperature-programmed reduction (TPR) of molybdenum oxides put forward the bulk MoO_3 cannot be reduced at 280 °C in H_2 atmosphere [53]. Therefore, we believe that the $MoO_xC_yH_z$ is formed

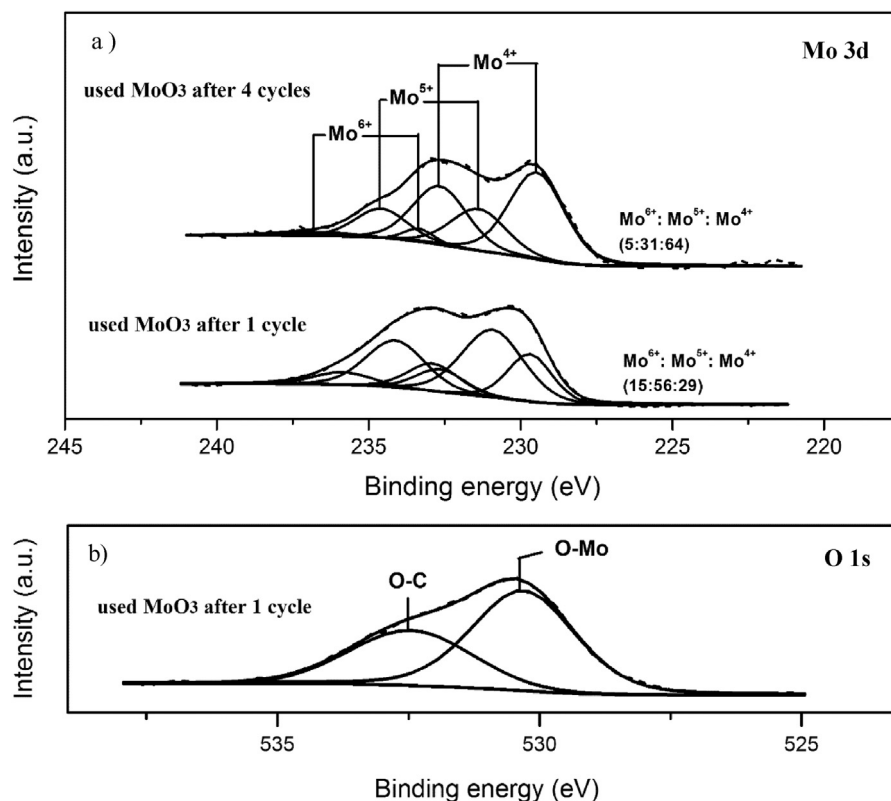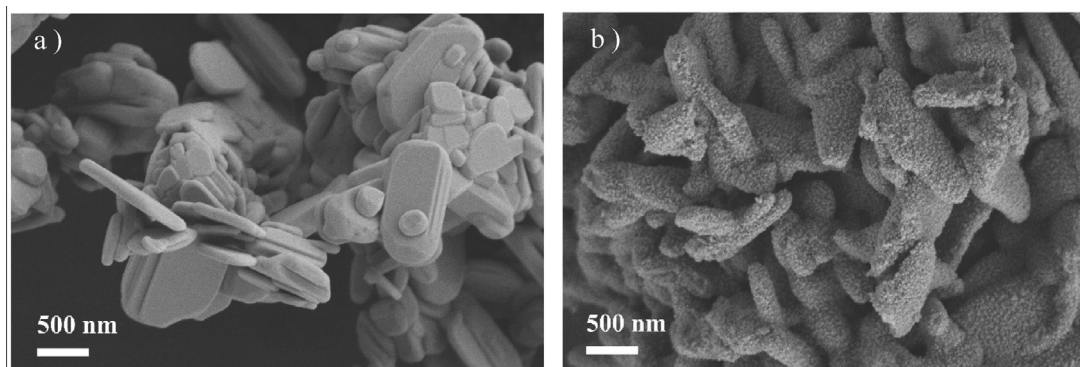with the assistance of active hydrogen species from the solvent. In touch with the massive active hydrogen offered by supercritical ethanol, MoO_3 reconstructed by shear planes, wherein new oxygen vacancies are created and then filled timely with systematic carbon atoms to form an oxycarbohydride phase that slows down the formation of inert MoO_2 [36,52]. For the non-alcohol solvents, the XRD of used catalysts show that MoO_3 was not reduced (Fig. 4), which indicates that there was a lack of the hydrogen sources.

Based on the active oxycarbohydride phase, the reason for different selective deoxygenation activity in alcohols arises. In Fig. 4, the XRD patterns of the used catalyst in ethanol, methanol and isopropanol are compared. The used catalyst in ethanol shows intense $MoO_xC_yH_z$ diffraction peaks, while the peak intensities of the phase are weakened distinctly for the spent catalyst in methanol. Even the used catalyst in isopropanol shows almost no $MoO_xC_yH_z$ phase and only a pattern of MoO_2. XPS spectra of all post-reaction samples were therefore acquired to probe the final Mo species states on the catalyst surface (Figs. 6a and S2), where 56%, 44% and 18% of Mo^{5+} was detected respectively for ethanol, methanol and isopropanol systems. Obviously, the decline of the deoxygenation capacity from ethanol to isopropanol is attributed to the decrease of the amount of stable active species with Mo^{5+} on the catalyst surface. Wang et al. [44] proposed that the ability of H-transfer of isopropanol is better than methanol and ethanol. Since the active hydrogen species from alcohol is considered as the main hydrogen source, the excessive reduction can result in the deficiency of $MoO_xC_yH_z$. Additionally, systematic carbon filling the oxygen vacancies of MoO_3 is the key step to form the $MoO_xC_yH_z$ phase [52]. The alcohol as a carbon source is important for the process. As a consequence, the ability of providing carbon atoms of the alcohol is also likely to influence the quantity of the stable Mo^{5+} active species.

On the other hand, we also try to illustrate the origin of methyl and ethyl groups, as well as the process of converting catechol to alkylphenols. The removal of hydroxyl group from ethanol molecules via the adsorption on metallic oxygen vacancies probably result in plentiful ethyl groups [33]. The existence of ethene, ethane and diethyl ether in the gaseous products (Table S1) certify the process is feasible. For methyl, we do not believe the methyl removed from guaiacol is the main methyl source for the substitutions due to the similar conversion results with catechol as the reactant (Scheme 2, Entry 28). Bouchy et al.[50] reported the electronic structure of Mo in $MoO_xC_yH_z$ was modified in the direction of the Pt structure, and the high selectivity to alkane isomerization

Fig. 6. XPS curves of a) Mo 3d of the used catalyst after 1 cycle and after 4 cycles b) O 1s of the used catalyst after 1 cycle at 280 °C in ethanol.
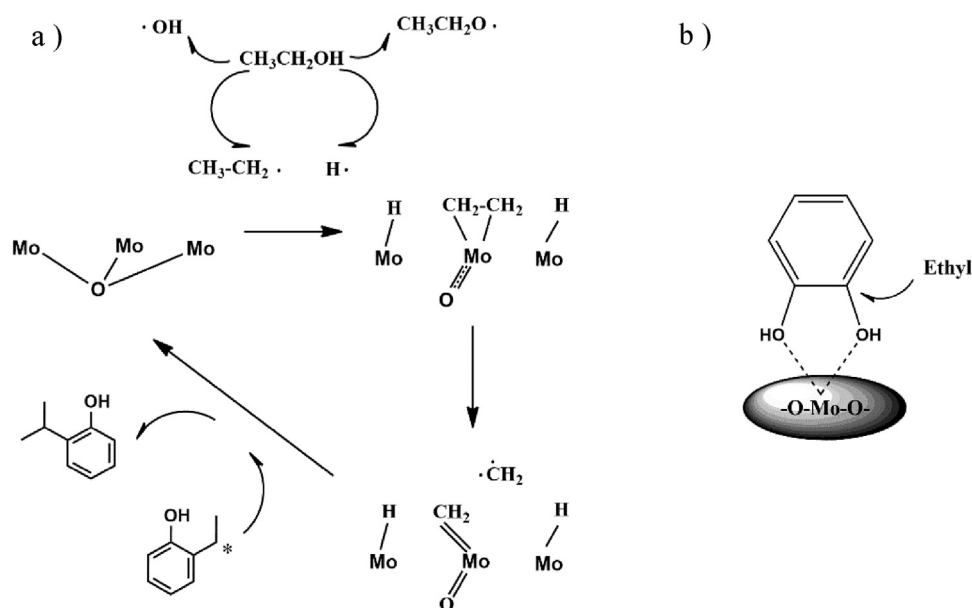

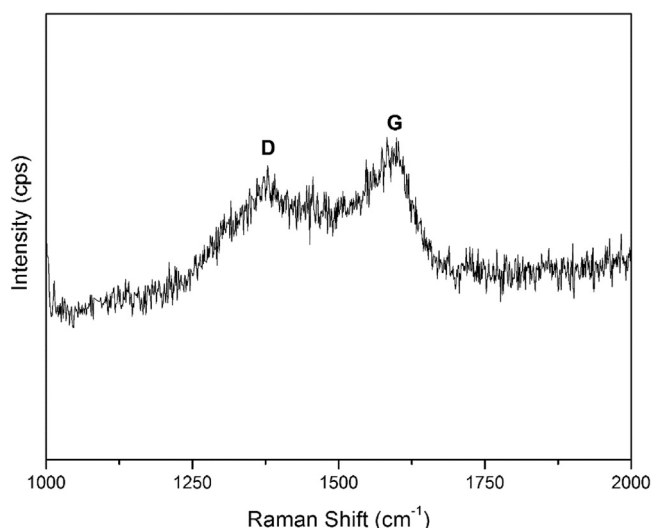**Fig. 7.** SEM micrographs of a) fresh MoO_3 and b) used MoO_3 after one cycle at 280 °C in ethanol.

was attributed to the interventional mechanism involving a metallacyclic intermediate, where available methyl was obtained. Thus, we speculate that the possible process for generation and substitution of methyl in the system is as Scheme 4a. When accessing to Mo atoms, ethyl and hydrogen species from ethanol can form metallacycles with Mo under the assistance of the high concentration of oxygen by trapping the excess of free electrons of Mo surface. After breakage of the metallacycles, methyl groups are created on metal atoms. The α-carbon of lower alkylphenol captures the methyl and gives off an activated hydrogen to form higher alkylphenol. Besides, we have proved that the interaction between two adjacent hydroxyl groups and the catalyst surface facilitates the conversion of catechol to alkylphenols. Considering the active species, its conceivable steps are that adjacent hydroxyl groups are adsorbed on the same metallic oxygen vacancy, which leads the formation of a pentabasic ring. Due to the effect of angle strain, it is easy to realize the breakage of Ar-OH bond and the substitution of alkyl groups (Scheme 4b).

3.7. Stability of MoO_3 catalyst

The reusability of the catalyst was tested with three extra runs. After each, the catalyst was recovered with filtration and used directly without treatment (Table 1, Entry 17–19). MoO_3 underwent a gradual deactivation with the conversion decreasing from 99% (1st cycle) to 34% (4th cycle). However, the catalytic activity can be completely recovered by calcining the catalyst at 600 °C for 2 h in air (Table 1, Entry 20). XPS analysis of the spent catalysts shows the Mo^{5+} in active species were reduced to Mo^{4+} partly from one cycle to four cycles with Mo^{5+} proportion decreasing from 56% to 31% and Mo^{4+} proportion increasing from 29% to 64% (Fig. 6a). On the other hand, the comparison of SEM micrographs between fresh MoO_3 and used MoO_3 after 1 cycle demonstrates the catalyst surface underwent an evolvement during the reaction period (Fig. 7a and b). The smooth morphology were replaced by rugged surface with tiny breadcrumbs-shaped particles. A certain amount of carbon element, except molybdenum and oxygen, was found

Scheme 4. The possible steps for a) generation and substitution of methyl and b) conversion of catechol to alkylphenols.

Fig. 8. Raman spectrum analysis of the used catalyst at 280 °C in ethanol.

using atomic mapping measurements (Fig. S3). That may be due to the formation of the oxycarbohydride phase by shared-plane reconstruction of MoO_3 or carbon deposition on the surface of the catalyst. Raman spectrum analysis further verifies both amorphous and graphite carbon coexist on the surface of the used catalyst in the ethanol system (Fig. 8). Hence, we conclude that the deactivation of MoO_3 is reversible and caused by the consumption of Mo^{5+} and deposition of carbon. These results agree with the findings reported by Shetty et al. for the stability of MoO_3 catalysts in a vapor-phase packed-bed down-flow reactor with hydrogen pressure [37].

4. Conclusions

The good activity of the MoO_3 catalyst in selective conversion of guaiacol to alkylphenols in supercritical ethanol was investigated. In addition to EPs, higher alkylphenols, *i.e.* IPPs, *tert-* and *sec-* BPs and TAP, are also produced. A total selectivity of 86% for the alkylphenols with a high conversion of 99% was achieved at 280 °C

for 4 h. Just for the quantified products, the alkylphenols account for about 94%, and six molecules, including 2,5-diethylphenol, 2,6-diisopropylphenol, 2,4-diisopropylphenol, 2,6-ditertbutylphenol, 2,4-ditertbutylphenol and 2,6-ditertbutyl-4-ethylphenol, were the main products. The catalyst has better performance in alcohols than in the other solvents. Ethanol is found to be the most effective alcohol solvent. Based on the results of control tests, we proposed the pathways of guaiacol to the higher alkylphenols. Catechol, as an intermediate, is formed firstly via demethylation of guaiacol and experiences a direct alkylation step to the EPs. The activated hydrogen on the α-carbon of EPs then be substituted consecutively by methyl and ethyl derived from the solvent, leading the formation of the higher alkylphenols. The catalyst characterization after reaction reveals an oxycarbohydride phase with Mo^{5+} is the active species in the catalytic process and that is formed with the assistance of active hydrogen species (not H_2) from supercritical ethanol. The different activities of deoxygenation in alcohols come from the different quantity of stable active species with Mo^{5+} formed on the catalyst surface. The MoO_3 catalyst undergoes gradual deactivation because of Mo^{5+} consumption and carbon deposition but can be regenerated completely with a simple calcination.

Appendix A. Supplementary data

Supplementary data associated with this article can be found, in the online version, at http://dx.doi.org/10.1016/j.apcatb.2017.08.009.

References

[1] Z. Joseph, P.C.A. Bruijnincx, A.L. Jongerius, B.M. Weckhuysen, Chem. Rev. 110 (2010) 3552–3599.
[2] C. Li, X. Zhao, A. Wang, G.W. Huber, T. Zhang, Chem. Rev. 115 (2015) 11559–11624.
[3] K. Barta, T.D. Matson, M.L. Fettig, S.L. Scott, A.V. Iretskii, P.C. Ford, Green Chem. 12 (2010) 1640–1647.
[4] R. Ma, W. Hao, X. Ma, Y. Tian, Y. Li, Angew. Chem. Int. Ed. 53 (2014) 7310–7315.
[5] X. Ma, Y. Tian, W. Hao, R. Ma, Y. Li, Appl. Catal. A 481 (2014) 64–70.
[6] X. Huang, T.I. Koranyi, M.D. Boot, E.J. Hensen, ChemSusChem 7 (2014) 2276–2288.
[7] A.K. Deepa, P.L. Dhepe, ACS Catal. 5 (2015) 365–379.
[8] X. Ma, K. Cui, W. Hao, R. Ma, Y. Tian, Y. Li, Bioresour. Technol. 192 (2015) 17–22.
[9] A. Narani, R.K. Chowdari, C. Cannilla, G. Bonura, F. Frusteri, H.J. Heeres, K. Barta, Green Chem. (2015) 5046–5057.
[10] V. Molinari, G. Clavel, M. Graglia, M. Antonietti, D. Esposito, ACS Catal. 6 (2016) 1663–1670.
[11] Y.Y. Wang, L.L. Ling, H. Jiang, Green Chem. 18 (2016) 4032–4041.
[12] F. Yan, R. Ma, X. Ma, K. Cui, K. Wu, M. Chen, Y. Li, Appl. Catal. B 202 (2017) 305–313.
[13] M.P. Pandey, C.S. Kim, Chem. Eng. Technol. 34 (2011) 29–41.
[14] V.N. Bui, D. Laurenti, P. Afanasiev, C. Geantet, Appl. Catal. B 101 (2011) 239–245.
[15] V.N. Bui, D. Laurenti, P. Delichère, C. Geantet, Appl. Catal. B 101 (2011) 246–255.
[16] A.L. Jongerius, R. Jastrzebski, P.C.A. Bruijnincx, B.M. Weckhuysen, J. Catal. 285 (2012) 315–323.
[17] A. Gutierrez, R.K. Kaila, M.L. Honkela, R. Slioor, A.O.I. Krause, Catal. Today 147 (2009) 239–246.
[18] C. Zhao, J. He, A.A. Lemonidou, X. Li, J.A. Lercher, J. Catal. 280 (2011) 8–16.
[19] C. Zhao, J.A. Lercher, ChemCatChem 4 (2012) 64–68.
[20] G. Yao, G. Wu, W. Dai, N. Guan, L. Li, Fuel 150 (2015) 175–183.
[21] M.V. Bykova, D.Y. Ermakov, V.V. Kaichev, O.A. Bulavchenko, A.A. Saraev, M.Y. Lebedev, V.A. Yakovlev, Appl. Catal. B 113–114 (2012) 296–307.
[22] R.N. Olcese, M. Bettahar, D. Petitjean, B. Malaman, F. Giovanella, A. Dufour, Appl. Catal. B 115–116 (2012) 63–73.
[23] T. Mochizuki, S.-Y. Chen, M. Toba, Y. Yoshimura, Appl. Catal. B 146 (2014) 237–243.
[24] L. Nie, P.M. de Souza, F.B. Noronha, W. An, T. Sooknoi, D.E. Resasco, J. Mol. Catal. A: Chem. 388–389 (2014) 47–55.
[25] L. Yang, W. Zhou, K. Seshan, Y. Li, J. Mol. Catal. A: Chem. 368–369 (2013) 61–65.
[26] L. Yang, Y. Li, P.E. Savage, Ind. Eng. Chem. Res. 53 (2014) 2633–2639.
[27] L. Yang, K. Seshan, Y. Li, Catal. Commun. 30 (2013) 36–39.
[28] R. Ma, K. Cui, L. Yang, X. Ma, Y. Li, Chem. Commun. 51 (2015) 10299–10301.
[29] V.M.L. Whiffen, K.J. Smith, Energy Fuels 24 (2010) 4728–4737.
[30] H.Y. Zhao, D. Li, P. Bui, S.T. Oyama, Appl. Catal. A 391 (2011) 305–310.
[31] I.T. Ghampson, C. Sepúlveda, R. Garcia, B.G. Frederick, M.C. Wheeler, N. Escalona, W.J. DeSisto, Appl. Catal. A 413–414 (2012) 78–84.
[32] I. Tyrone Ghampson, C. Sepúlveda, R. Garcia, J.L. García Fierro, N. Escalona, W.J. DeSisto, Appl. Catal. A 435–436 (2012) 51–60.
[33] T. Prasomsri, T. Nimmanwudipong, Y. Román-Leshkov, Energy Environ. Sci. 6 (2013) 1732–1738.
[34] D.J. Rensel, S. Rouvimov, M.E. Gin, J.C. Hicks, J. Catal. 305 (2013) 256–263.
[35] W.S. Lee, Z. Wang, R.J. Wu, A. Bhan, J. Catal. 319 (2014) 44–53.
[36] T. Prasomsri, M. Shetty, K. Murugappan, Y. Román-Leshkov, Energy Environ. Sci. 7 (2014) 2660–2669.
[37] M. Shetty, K. Murugappan, T. Prasomsri, W.H. Green, Y. Román-Leshkov, J. Catal. 331 (2015) 86–97.
[38] L. Seguin, M. Figlarz, R. Cavagnat, J.C. Lassègues, Spectrochim. Acta Part A 51 (1995) 1323–1344.
[39] T. Matsuda, Y. Hirata, F. Uchijima, H. Itoh, N. Takahashi, Bull. Chem. Soc. Jpn. 73 (2000) 1029–1034.
[40] W. Chen, Z. Luo, C. Yu, Y. Yang, G. Li, J. Zhang, Fuel Process. Technol. 126 (2014) 420–428.
[41] X. Huang, T.I. Korányi, M.D. Boot, E.J.M. Hensen, Green Chem. 17 (2015) 4941–4950.
[42] Q. Song, F. Wang, J. Cai, Y. Wang, J. Zhang, W. Yu, J. Xu, Energ. Environ. Sci. 6 (2013) 994–1007.
[43] S.J. Blanksby, G.B. Ellison, Acc. Chem. Res. 36 (2003) 255–263.
[44] X. Wang, R. Rinaldi, Energ. Environ. Sci. 5 (2012) 8244–8260.
[45] Y. Luo, Handbook of Bond Dissociation Energies in Organic Compounds, vol. 4, CRC Press LLC, Boca Raton, 2003, p. 105.
[46] D.A. Robaugh, S.E. Stein, Int. J. Chem. Kinet. 13 (1981) 445–462.
[47] A.L. Jongerius, R.W. Gosselink, J. Dijkstra, J.H. Bitter, P.C.A. Bruijnincx, B.M. Weckhuysen, ChemCatChem 5 (2013) 2964–2972.
[48] G.D.L. Puente, A. Gil, J.J. Pis, P. Grange, Langmuir 15 (1999) 5800–5806.
[49] C. Bouchy, C. Pham-Huu, B. Heinrich, E.G. Derouane, D.A. Hamid, M.J. Ledoux, Appl. Catal. A 215 (2001) 175–184.
[50] C. Bouchy, C. Pham-Huu, B. Heinrich, C. Chaumont, M.J. Ledoux, J. Catal. 190 (2000) 92–103.
[51] X. Ma, R. Ma, W. Hao, M. Chen, F. Yan, K. Cui, Y. Tian, Y. Li, ACS Catal. 5 (2015) 4803–4813.
[52] P. Delporte, F.D.R. Meunier, C. Pham-Huu, P. Vennegues, M.J. Ledoux, J. Guille, Catal. Today 23 (1995) 251–267.
[53] P. Arnoldy, J.C.M.D. Jonge, J.A. Moulijn, J. Phys. Chem. 89 (1985) 4517–4526.